Tracking the Fate of Therapeutic Proteins Using Ratiometric Imaging of Responsive Shortwave Infrared Probes

Pradeep Shrestha,[1] Nimit L. Patel,[2] Joseph D. Kalen,[2] Syed Muhammad Usama,[1,3*] and Martin J. Schnermann[1*]

[1] Chemical Biology Laboratory, Center for Cancer Research, National Cancer Institute, Frederick, Maryland 21702, United States

[2] Small Animal Imaging Program, Frederick National Laboratory for Cancer Research, Leidos Biomedical Research Inc., Frederick, Maryland 21702, United States

[3] Department of Chemistry, The University of Texas at San Antonio, San Antonio, Texas 78249, United States

KEYWORDS antibody drug conjugate, fluorogenic probes, shortwave infrared, optical imaging, linker chemistry

ABSTRACT: Monoclonal antibodies (mAbs) are essential agents for cancer treatment and diagnosis. Advanced optical imaging strategies have the potential to address specific questions regarding their complex *in vivo* life cycle. This study presents responsive shortwave infrared (SWIR) probes and an associated imaging scheme to assess mAb biodistribution, cellular uptake, and proteolysis. Specifically, we identify a Pegylated benzo-fused norcyanine derivative (Benz-NorCy7) that is activated in acidic environments and can be appended to mAbs without significant changes in optical properties. As a mAb conjugate, this agent shows high tumor specificity in a longitudinal imaging study in a murine model. To enable independent tracking of mAb uptake and lysosomal uptake and retention, a two-color ratiometric imaging strategy was employed using an "always-ON" heptamethine cyanine dye (λ_{ex} = 785 nm) and the pH-responsive Benz-NorCy7 (λ_{ex} = 890 nm). To assess proteolytic catabolism, we append a cleavable carbamate to Benz-NorCy7 to create turn-ON probes. These agents facilitate the comparison of two common peptide linkers and provide insights into their *in vivo* properties. Overall, these studies provide a strategy to assess the fate of protein-based therapeutics using optical imaging in the SWIR range.

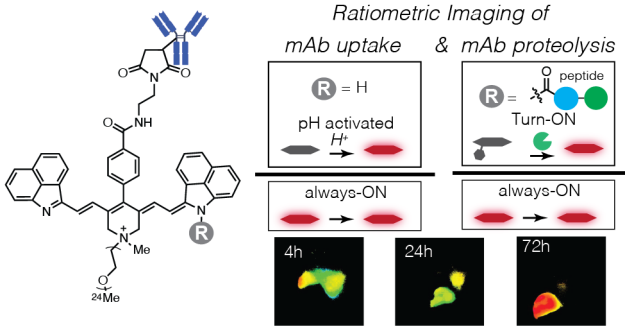

INTRODUCTION

Monoclonal antibodies (mAbs) and their conjugates are indispensable therapeutics and diagnostics.[1] For preclinical use, the combination of mAbs and fluorescent small molecules find broad use for target protein visualization and quantification. In a clinical setting, fluorophore-labeled mAbs enable fluorescence-guided surgical (FGS) procedures.[2,3] Furthermore, *in vivo* optical imaging can provide critical insights that can guide the design of future antibody therapies.[4,5] Single-color strategies only address biodistribution, which can also be assessed with radiolabeling strategies.[6,7] However, unlike radiolabeling, optical probes can respond to biological stimuli and be used in combination when excited at discrete wavelengths to enable multicolor imaging.[8] These strategies have the potential to assess local chemical environments encountered by mAbs *in vivo*, which might inform both their design and use. However, further probe discovery efforts are needed to facilitate such studies.

In vivo optical imaging has been bolstered by the application of NIR (700-900 nm) and, more recently, SWIR (1000-1500 nm) wavelengths. NIR probes are essential components of fluorescence-guided surgery (FGS) strategies, and a number of targetable and responsive probes are available in this range. [2,9-14] SWIR imaging efforts have been enabled by the observation that indocyanine green (ICG), and related heptamethine cyanines, provide a meaningful long wavelength emission (>1000 nm) that improves imaging resolution in complex settings.[15-18] Adding longer wavelength absorbing/emitting agents facilitates multicolor *in vivo* imaging, and there have been significant strides towards this goal using targeted and non-targeted always-ON probes.[19-23] In addition, several chemistries have been identified that create responsive probes in the SWIR range.[24] However,

https://doi.org/10.26434/chemrxiv-2024-zc58k **ORCID:** https://orcid.org/0000-0002-0503-0116 Content not peer-reviewed by ChemRxiv. **License:** CC BY-NC-ND 4.0

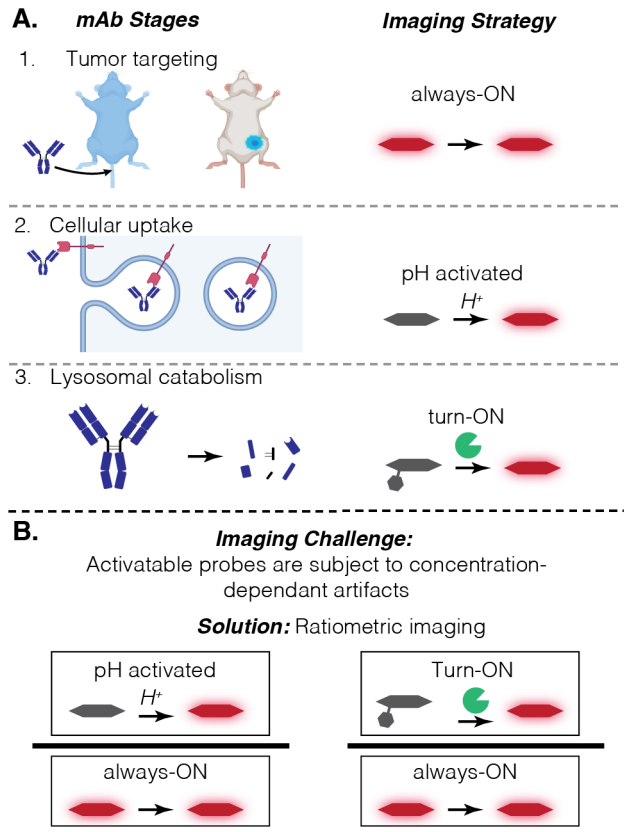

Figure 1: A. mAb stages during *in vivo* tumor targeting and associated imaging strategy. **B.** Ratiometric scheme to correct for concentration-dependent artifacts.

existing activatable SWIR probes are too hydrophobic to be incorporated into protein-targeted imaging strategies.[5]

Interrogating the discrete environments encountered by therapeutic proteins could address questions about their *in vivo* life cycle. In the case of tumor targeting mAbs, there are three stages that would ideally be distinguished: (1) a localization phase that includes initial circulation, tumor penetration, and target antigen binding, (2) transit through the endosomal pathway, and (3) protein catabolism, which occurs primarily in the lysosome.[25] While the first stage is characterized by changes in spatial distribution, the latter two are best assessed using chemical features - pH and proteolysis, respectively (Figure 1A). Therefore, while biodistribution can be evaluated with always-ON probes, assessing pH and proteolysis requires the use of responsive probes that are activated by acidic pH and the bond cleavage. A fundamental challenge inherent in the use of isolated responsive probes is that probe concentration cannot be separated from probe activation. Notable, this issue is particularly acute for *in vivo* imaging of long circulating, slow accumulating mAbs, which also leads to animal-to-animal variations. To imaging this complex process, prior studies using either FRET pairs, or less commonly ratiometric imaging, have been developed using conventional visible or NIR probes.[26-29] We hypothesized that two color ratiometric strategies using purpose-built optical imaging probes and SWIR imaging could provide unique insights and improved quantitation(Figure 1B).

This study details steps towards a general strategy to track *in vivo* protein fate. We identify an aggregation-resistant pegylated benzo-fused norcyanine that emits in the SWIR range only in an acidic environment (pKa =5.3). When appended to a therapeutic mAb, the agent enables tumor-selective imaging with an exceptional tumor-to-background ratio (TBR). Two-color ratiometric imaging using an excitation-based multiplexing approach allow for independent monitoring of tumor uptake/targeting and lysosomal uptake in murine models, allowing for concentration-corrected measurements of antibody internalization. To assess lysosomal catabolism *in vivo*, we modify this probe with a cleavable peptidic linker. The resulting proteolysis-responsive compounds were used to compare the *in vivo* cleavage propensity of two common antibody-drug conjugate (ADC) peptide-based linkers. Overall, these studies provide a high resolution means to quantitatively assess tumor targeting, cellular uptake and protein catabolism longitudinally in murine models.

RESULTS AND DISCUSSION

Probe Discovery – Norcyanines are a unique class of cyanines, that lack alkylation on the indolenine nitrogens, which renders them pH sensitive and suitable for pH-responsive imaging.[30,31,32] To improve the physical properties of the otherwise quite hydrophobic benzo-fused norcyanines, we previously reported the use of quaternary nitrogen in central ring system – a strategy informed by prior cyanine modification efforts.[33,34] The design of the optimized benzo-fused norcyanine pH probe used here entailed a subtle but ultimately critical modification to the prior compound, which was used previously only for untargeted pH imaging Specifically, the PEG_4 derivative prepared previously exhibited dramatic pH responses and formed red-shifted

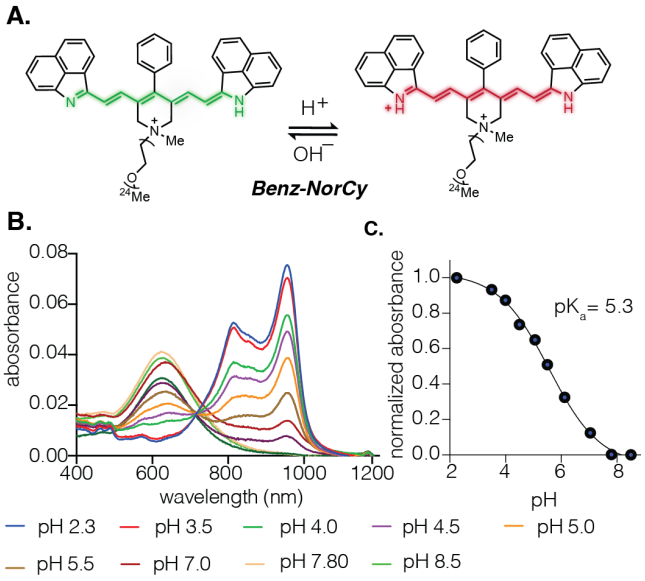

Figure 2: A. Structure and activation mechanism of **Benz-NorCy7**. **B**. Absorbance of **Benz-NorCy7** at various pHs (Britton-Robinson buffers) C. p*K*a curve (normalized absorbance at 956 nm).

https://doi.org/10.26434/chemrxiv-2024-zc58k **ORCID:** https://orcid.org/0000-0002-0503-0116 Content not peer-reviewed by ChemRxiv. **License:** CC BY-NC-ND 4.0

aggregates in aqueous solution.[35] However, derivatives of this compound could not be employed effectively as antibody conjugates, as described in more detail below. We hypothesized that simply increasing the length of the PEG chain could address this limitation. To test this, the corresponding PEG_{24} variant (**Benz-NorCy7**) was accessed through a similar sequence to that described previously (see supplemental information). The compound exhibited the pH response expected from a norcyanine derivative. Specifically, it displayed a blue-shifted absorbance maximum (λ_{max} = 628 nm) in basic and neutral pHs, but the characteristic cyanine red-shifted absorbance with λ_{max} = 956 nm in acidic pH (Figure 2A, Figure S1). Furthermore, while the previous compounds formed complex bathochromic and hypsochromic aggregates in phosphate buffer,[35] no such behavior was observed for **Benz-NorCy7**, with titration of the λ_{max} providing a p*K*a of 5.3 (Figure 2B,C). Critically, this pKa is well below that of even the acidic tumor microenvironment and, consequently, the probe will largely be activated only in lysosomal compartments. The long wavelength emissive properties of the protonated species were also assessed. The fluorescence quantum yield (Φ_F) of 0.14% (EtOH w/ 1% TFA) and emission maxima of 996 nm are similar to other SWIR probes that have found significant use for *in vivo* imaging.[22,36,37] We also carried out initial toxicity and stability measurements, suggesting the compound is stable across a range of pHs, as well as in serum, and is well tolerated by cells (Figure S2).

To enable antibody-targeted imaging, we prepared a maleimide derivative of **Benz-NorCy7**, which was conjugated to Panitumumab (Pan) using hinge disulfide cysteine labeling to yield **Pan-Benz-NorCy7-pH** following size exclusion chromatography purification (Figure S3). Pan is a therapeutic antibody that binds to the epidermal growth factor receptor (EGFR) and then is ultimately internalized to the lysosome.[38]

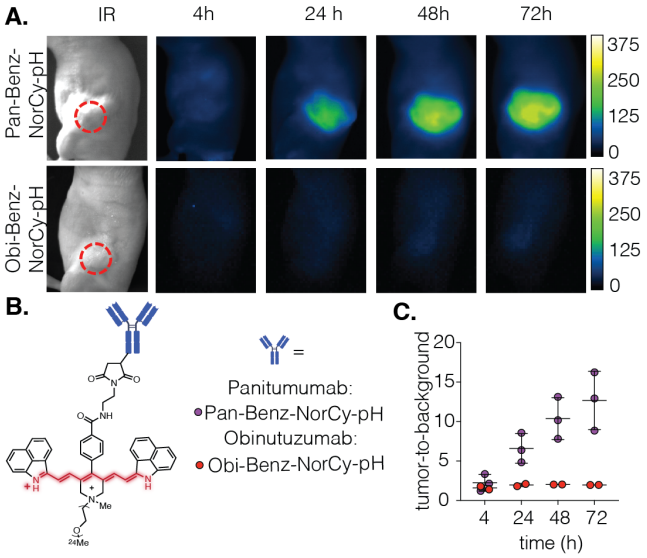

Figure 3. A. Fluorescent images following the injection of Pan-Benz-NorCy7-pH (200µg, DOL 4) in female athymic nude mice (n = 3) with JIMT-1 tumors at 4, 24, 48, and 72 h time points **B.** Structure of **Pan-Benz-NorCy7-pH** and **Obi-Benz-NorCy7-pH** **C.** Quantification of the tumor to background ratio of **Pan-Benz-NorCy7-pH** and **Obi-Benz-NorCy7-pH** at different time points.

Pan-Benz-NorCy7-pH (200 µg, i.v.) was administered to female athymic nude mice bearing tumors derived from JIMT-1 cells injected orthotopically in the lower inguinal mammary fat pad (MFP, 250–350 mm^3). Subsequently, the mice underwent imaging at 4, 24, 48, and 72 h post-injection using a custom SWIR imaging instrument (Figure S4). Using an 890 nm-excitation laser with a 960 nm long pass emission filter, the **Pan-Benz-NorCy7-pH** probe exhibited remarkable tumor specificity, resulting in a significantly enhanced tumor-to-background ratio (TBR) of ~13 with minimal background signal observed 72 h post-administration. Notably, the TBR at 24 h (~ 6.5), matches that obtained with conventional probes at 48-72 h (Figure S4), suggesting high quality imaging can be obtained at earlier time-points with this pH-activatable strategy.[39,40] To examine the role of receptor-mediated uptake, we conducted control experiments using an isotype control, Obinutuzumab (Obi), a humanized anti-CD20 monoclonal antibody that should not have a cognate target in this model. **Obi-Benz-NorCy7-pH** exhibited minimal activation within the tumor, indicating that the observed signal with **Pan-Benz-NorCy7-pH** is due to EGFR-specific binding JIMT-1 tumors (Figure S5). This activatable pH-responsive probe could find application in optical-guided surgical procedures where high-contrast, early time point imaging is desirable.

Ratiometric Imaging - Single-color imaging cannot distinguish between the effects of probe activation and increased tumor concentration. To separate these features, we envisioned using a ratiometric two-color imaging strategy.[41] Previous studies established an excitation-based multiplexing scheme for SWIR imaging, wherein only the excitation wavelength is altered, and multiple channels are obtained using a single long-pass emission filter.[19,21] Here, we aimed to extend this approach to responsive two-color imaging. For the "always-ON" 780 nm channel, we chose the heptamethine cyanine dye, **FNIR-Tag-766**, which has been optimized for efficient protein labeling and tumor targeting.[40] This approach then allows us to use the 890 nm excitation channel for the responsive **Benz-NorCy7** agent, which can be assessed either independently or as a ratio with the 785 channel. We first conducted phantom imaging using an equimolar mixture of **FNIR-Tag-766** and **Benz-NorCy7-pH**. This revealed orthogonal emission, with limited overlap (<1% and 11%) when excited at 785 nm for **FNIR-Tag-766** (1 ms excitation) and 890 nm for **Benz-NorCy7-pH** (50 ms excitation). We then found that a 50:1 mixture of **Benz-NorCy7-pH** and **FNIR-Tag-766** (in pH 4.5 phosphate buffer) yielded similar emission intensities under identical exposure times, also with measurable interchannel crosstalk (16 and 19%) (Figure S6). However, as anticipated, the issues of channel separation are corrected for through ratiometric processing and do not impact pH imaging. Specifically, we found that the 785 channel showed no pH dependence in the mixture, while excitation at 890 nm resulted in a sigmoidal pH response. This could be visualized in an 890/785 16-color format image of the mixture (Figure 4A-D). These phantom studies support the hypothesis that the two different excitation wavelengths can be used independently, with the 785 and 890 nm channels employing the always-ON and responsive components, respectively.

https://doi.org/10.26434/chemrxiv-2024-zc58k **ORCID:** https://orcid.org/0000-0002-0503-0116 Content not peer-reviewed by ChemRxiv. **License:** CC BY-NC-ND 4.0

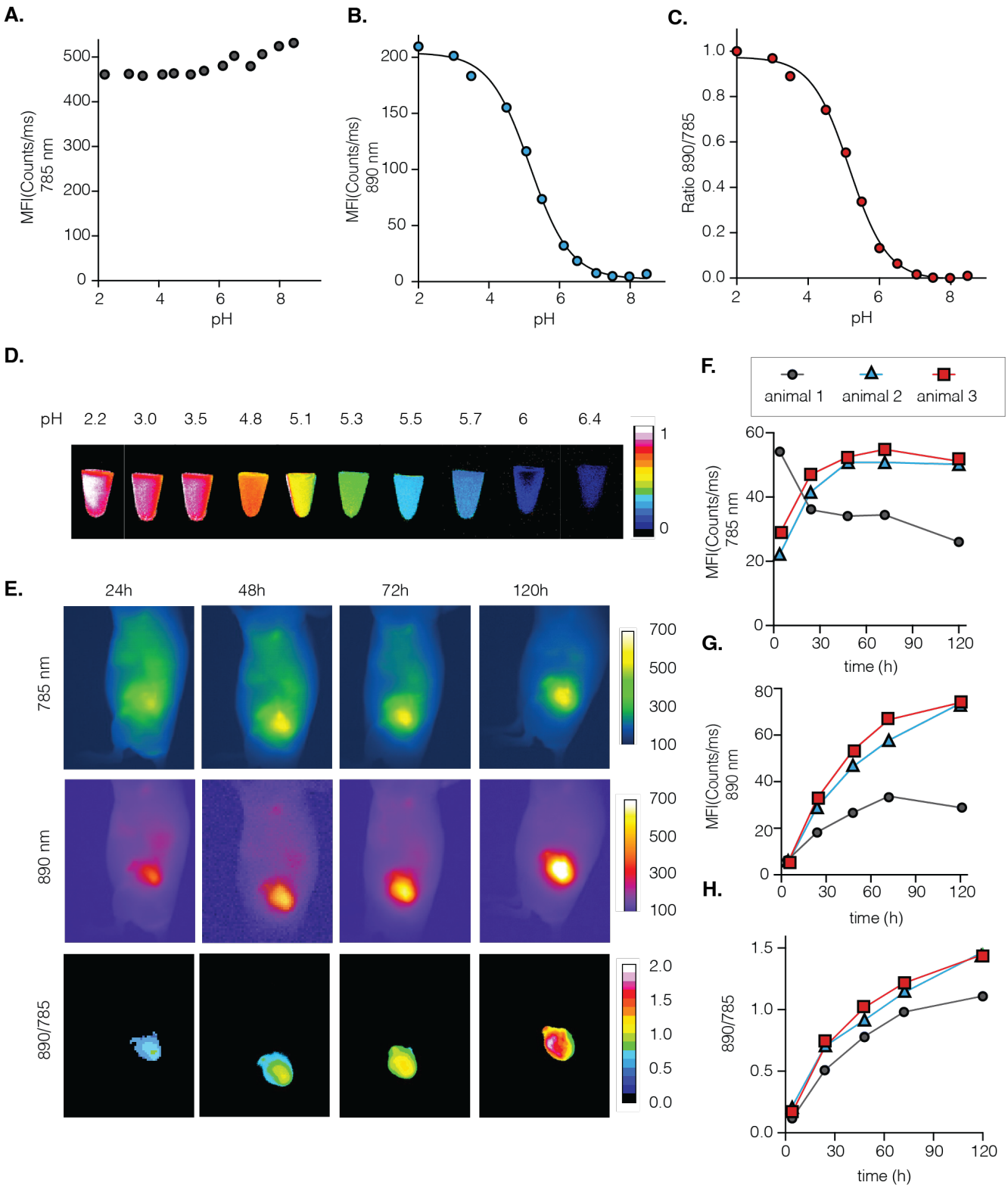

Figure 4 Quantification of emission intensity (> 960 nm) obtained from phantom imaging of a 1:50 ratio of **Pan-FNIR-Tag-766**: **Pan-Benz-NorCy7-pH** in different pH buffers with **A.** 785 excitation and **B**. 890 excitation and **C**. a normalized 890/785 nm emission ratio **D.** 890/785 ratio at different pH ranges obtained from phantom imaging represented with pH response in a 16-color format. **E**. Two color imaging following the injection of a mixture of **Pan-Benz-NorCy7-pH** and **Pan-FNIR-Tag-766** in in female athymic nude mice (n=3) with JIMT-1 tumors at 4, 24, 48, 72 and 120 h time points (200 µg, ratio of the two imaging probes = 1:50). **F**. Quantification of tumor emission at 785 nm channel at indicated time points **G**. Quantification of tumor emission at 890 nm channel at indicated time points. **H**. Ratio of 890/785 channels at tumor in indicated time points.

https://doi.org/10.26434/chemrxiv-2024-zc58k **ORCID:** https://orcid.org/0000-0002-0503-0116 Content not peer-reviewed by ChemRxiv. **License:** CC BY-NC-ND 4.0

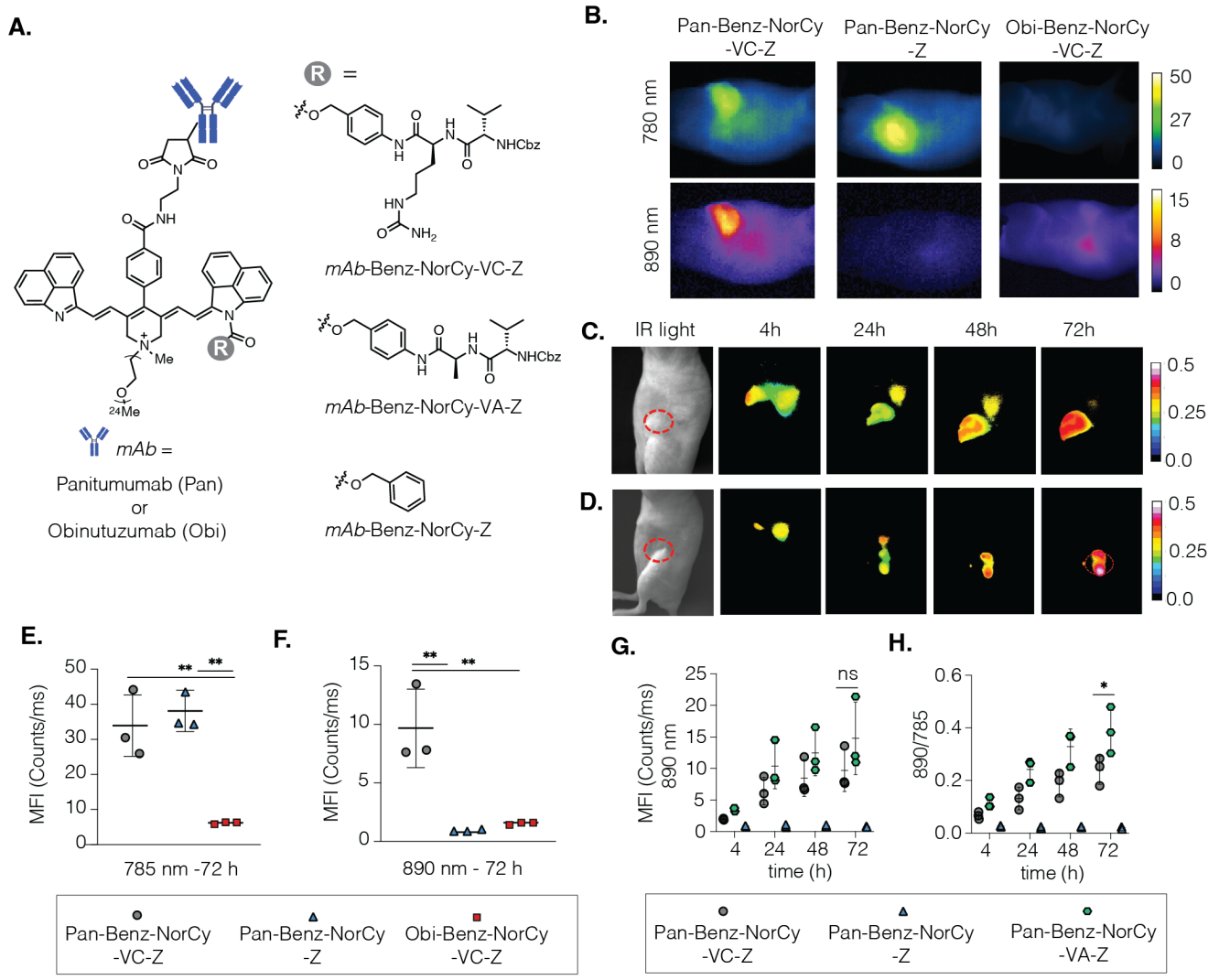

Figure 5 **A.** Structure of Panitumumab conjugates used in the animal study **B.** 785 and 890 nm excitation images of JIMT-1 tumor-bearing mice injected with **Pan-BenzNorCy-VC-Z: Pan-FNIR-Tag-766**, **Pan-Benz-NorCy-Z: Pan-FNIR-Tag-766** and **Obi-Benz-NorCy-VC-Z: Obi-FNIR-Tag-766** in female athymic nude mice (n=3) with JIMT-1 tumors imaged at 4, 24, 48, and 72h time points (200 µg, ratio of the two imaging probes = 1:50). **C**. Example of ratiometric imaging of **Pan-BenzNorCy-VC-Z: FNIR-Tag-766** at indicated time points. **D**. Example of ratiometric imaging of tumor for **Pan-BenzNorCy-VA-Z: FNIR-Tag-766** at indicated time points. Emission intensity from tumors at 72 h in 785 channel (**E**) and 890 nm (**F**) after injection with **Pan-BenzNorCy-VC-Z: Pan-FNIR-Tag-766**, **Pan-Benz-NorCy-Z: Pan-FNIR-Tag-766**, **and Obi-Benz-NorCy-VC-Z: Obi-FNIR-Tag-766**. **G.** Change in MFI over tumor in 890 channel for indicated groups and time points. **H**. Change in MFI in 890/785 ratiometric images for indicated groups and time points. Data points are displayed as mean ± SD, and the *p*-values were evaluated by the Student's *t*-test (ns *p*-value> 0.05, * *p*-value ≤0.05, ** *p*-value ≤0.01).

Imaging mAb Internalization - We envisioned applying this two-color imaging strategy to differentiate between mAb targeting/localization and internalization. Female athymic nude topically in the lower inguinal mammary fat pad (MFP) (250–350 mm^3) received intravenous (*i.v.*) or intratumoral (*i.t.*) injection of a mixture containing **Pan-Benz-NorCy7-pH** and **Pan-FNIR-Tag-766** (200 µg as a 50:1 ratio) (Figure S7), and imaging was conducted at 4-, 24-, 48-, 72-, and 120-h post-injection. We first analyzed the individual channels and found a nearly identical TBR values for the 890 channels to that obtained in the single-color imaging study (Figure S8-S9). This observation supports the orthogonality of the two channels and that co-injection appears to not alter targeting or cellular internalization. Analysis of the SWIR images obtained from the 785 nm and 890 nm channels revealed time-dependent variations in signal intensity. The half-life for tumor localization ($t_{1/2}$ = 10.5 h) of the always-ON 785 channel) is similar to that observed for the uptake $t_{1/2}$ measured with other optical and radiolabeling strategies.[27,42] By contrast, the ratiometric 890/785 channel exhibits a longer half-life ($t_{1/2}$ = 34.6 h). Using an *i.v.* injection, this number represents the time required for tumor localization and lysosomal uptake. By contrast, intratumoral *(i.t.)* injection

https://doi.org/10.26434/chemrxiv-2024-zc58k **ORCID:** https://orcid.org/0000-0002-0503-0116 Content not peer-reviewed by ChemRxiv. **License:** CC BY-NC-ND 4.0

eliminates the requirement for tumor localization, and isolates the time course of lysosomal uptake. Consistent with this assumption, an initial *i.t.* injection study obtains a shorter half-life ($t_{1/2}$ = 22.6 h) in the 890/785 channel (Figure S10-S11). Of note, the final ratio of the 890/785 (1.34 ± 0.20 at 72 h) is higher than that obtained upon phantom imaging, potentially due to improved tissue penetration of the 890 nm excitation/emission scheme.

An outcome of this approach is that the two-color strategy provided a means to address issues of animal variability. One of the animals (animal 1, Figure 4F,G) exhibited significantly lower emission intensity at 785 nm and 890 nm channels, which we hypothesize might be due to an unusually necrotic tumor in this animal. However, analysis of ratiometric images (890/785 nm) of all three animals gives a similar one-phase curve (Figure 4H). Overall, these data suggest that the ratiometric imaging strategy used here can directly assess lysosomal uptake, while correcting for issues of animal-to-animal variability.

Imaging mAb Catabolism - Upon internalization into the lysosome, the mAb enters an environment with high proteolytic activity. This process has been exploited through the development of protease-cleavable linker chemistries, which find broad use in antibody-drug conjugates (ADCs).[43,44] The ability to quantify and precisely capture the extent of linker cleavage, particularly in *in vivo* models, would enable improved comparison of various cleavable linkers. In prior work, we appended responsive functional groups onto the NIR norcyanine scaffold through a carbamate linkage leading to cyanine carbamate (CyBam) imaging agents.[45] When coupled with antibodies, these probes facilitated targeted imaging and enabled quantitative comparison of various cleavable linkers, although only in a single-color format. To enable a ratiometric variant of this approach, we envisioned using a targetable SWIR norcyanine carbamate as the responsive component.

We first examined linker positioning and the requirements of the norcyanine agent. In our prior work the antibody was attached to the probe through a cleavable linker, and we initially tested a related approach (see Figure S12-S13 for photophysical properties and structures). We obtained measurable tumor signal only with a high dose of antibody-dye conjugates (500 µg, Figure S14). This result may suggest that the liberated probe is not retained efficiently within the tumor. We also tested the PEG_4 compound and found that the compound predominantly yielded hepatic signals, highlighting the critical role of the PEG_{24} modification.[5,46,47] Critically, the pH imaging studies above suggest that placing the mAb attachment point directly onto the probe through the mesomeric aryl group may offer certain advantages, leading us to test a related approach for the activatable probes.

Using the aryl ring modification design strategy, the activatable probes were synthesized by modifying the conjugatable **Benz-NorCy7-pH** with either protease-cleavable linkers or a control benzyl carbamate. With access to these probes, we first validated that activation occurs in a binding- and linker-dependent fashion. The maleimides underwent efficient antibody labeling to yield **Pan-Benz-NorCy-VC-Z** and **Pan-Benz-NorCy-Z**, as well as the non-targeting control **Obi-Benz-NorCy-Z** (Figure 5A, Figure S15). Animal studies were conducted via *i.v* injection of the antibody-probe conjugate (200 µg with 2% of **Pan-FNIR-Tag-766**), and images were obtained 4, 24, 48, and 72 h post-injection (Figure 5B). We also corroborated the *in vivo* imaging results with *ex vivo* imaging of excised liver and tumor tissues, which was performed 72 h post injection. In assessing the always-ON 785 nm channel, only the EGFR-targeting Pan conjugates exhibited a significant tumor signal and not the control Obi conjugates (Figure 5E, Figure S16-S19). With respect to the activatable 890 channel, the **Pan-Benz-NorCy-VC-Z**, and not the **Pan-Benz-NorCy-Z** control probe, exhibited time-dependent improvement, while no signal was observed **Obi-Benz-NorCy-VC-Z** conjugate (Figure 5F, Figure S20). Critically, the absolute value of the 890 nm intensity is significantly lower (5-10%) than that seen with the pH imaging studies described above. These results demonstrate that probe activation requires both antibody binding and a cleavable linker for significant signal.

This SWIR-based imaging approach, particularly in the ratiometric format, enables the identification of spatial resolved patterns that have the potential to provide biological insights. For example, there is a clear hepatic signal at 4 h, that then disappears with increased tumor signals over time using the ratiometric approach (Figure 5C). While hepatic signals are apparent in some NIR imaging, the signal is more clearly resolved using the SWIR-based imaging approach. In addition, significant variation and spatially resolvable regions can be seen across the tumor (Figure 5D). Analysis of these variations suggests that they arise to a greater degree due to the 890 nm turn-ON channel, which may be due to necrotic regions or other features that lead to altered linker catabolism (Figure S21).

We hypothesized this approach might enable the comparison of two common dipeptide linkers used in the ADC field, Val-Cit and Val-Ala. While the former (Val-Cit) has been applied broadly, including in the approved ADC Adcetris, the latter (Val-Ala) has been explored in more recent ADC development efforts.[48] While exhibiting slightly reduced enzymatic cleavage kinetics, the Val-Ala dipeptide has been shown to provide improved *in vivo* stability and, in several cases, significantly enhanced *in vivo* efficacy.[49-53] Both of these compounds were imaged in an identical study as described above (Figure S22). In the 890 nm intensity data, there was no significant difference between the Val-Ala and Val-Cit variants, although a slight trend favoring the Pan-Val-Ala appears possible. By contrast, by incorporating the 785 nm always-ON channel to create the ratiometric images, the Val-Ala is activated to a statistically greater extent at both the 48 and 72 h time points. We hypothesize this improvement is due to corrections for animal-to-animal variations in tumor size and mAb avidity. The improvements in Val-Ala signal may be due to enhanced serum stability and/or altered physiochemical properties, though additional studies to better understand these subtle chemical issues are needed.

CONCLUSIONS

Here we develop activatable SWIR probes and apply them to investigate mAb targeting, internalization, and proteolysis. By optimizing the PEG substituent, a benzo-fused norcyanine (**Benz-NorCy7**) is identified that doesn't undergo complex aggregation in water or upon mAb labeling. When used in isolation, the resulting mAb conjugate enables exceptionally high contrast tumor imaging at early time points, which may have

https://doi.org/10.26434/chemrxiv-2024-zc58k **ORCID:** https://orcid.org/0000-0002-0503-0116 Content not peer-reviewed by ChemRxiv. **License:** CC BY-NC-ND 4.0

utility in guided surgical imaging procedures. A two-color imaging strategy distinguishes between mAb uptake and lysosomal activity, and addresses issues of animal-to-animal variability. Modification of this agent with protease-cleavable linkers facilitates *in vivo* imaging of catabolic activity, allowing for the quantitative comparison of two commonly used linkers used by the ADC community. A feature of this study is that the pH and protease-cleavable studies were carried out in an identical fashion, allowing for initial quantification of the degree of linker cleavage proteolysis. Differences in the absolute intensity of the 890 nm activatable channel would appear to suggest that ~5-10% of the linker units are cleaved over the first 72 h, which is similar to results obtained from other linker quantification efforts.[54,55]

Several aspects of this approach require additional comment. We have chosen to use mixtures of the always-ON and activatable probe mAb conjugates. This approach serves to normalize the activatable probe channel to an agent with optimal uptake. Another option would have been to append both probes on the same antibody. This approach would provide an internal reference with the potential to improve pH mapping and also to provide insight on the uptake and clearance of the doubly modified antibodies. Future studies that compare these options directly are likely merited. However, the disparity in brightness between the always-ON and the currently available responsive probes reported here make the dual labeling approach challenging to implement. Consequently, the identification of brighter long wavelength responsive probes, as well as the creation of flexible concentration-independent imaging strategies to apply them, remains an important goal.

Overall, these studies provide a new option for studies applying optical imaging to assess mAbs and ADCs in complex settings.[56] These studies have compared peptidic linkers and could also be applied to strategies that rely on other linker cleavage chemistries.[43] In addition, this approach could enable efforts to study agents that modulate the rate and extent of mAb internalization.[57,58] With respect to the probe chemistry, it is quite possible that slightly increasing the p*K*a of these compounds might improve their *in vivo* photon output. Additionally, probe development efforts that enable three-color imaging efforts might facilitate additional insight. In sum, these efforts add to the potential utility of *in vivo* optical imaging to guide the design and implementation of targeted therapeutic agents.

ASSOCIATED CONTENT

Supporting Information

This material is available free of charge via the internet at http://pubs.acs.org. Supporting Information contain synthesis procedure and characterization of key compounds and intermediate compounds, photophysical properties, details of in vivo experiments and supporting figures and tables.

AUTHOR INFORMATION

Corresponding Authors

* Email: syedmuhammad.usama@utsa.edu

* Email: martin.schnermann@nih.gov

Author Contributions

The manuscript was written through the contributions of all authors. All authors have given approval to the final version of the manuscript.

ABBREVIATIONS

NIR, near-infrared; ADC, Antibody Drug Conjugate; mAb, monoclonal antibody; PBS, phosphate buffer saline;; IVIS, *in vivo* imaging system; EGFR, epidermal growth factor; abs, absorbance; ex, excitation; em, emission; N.A, numerical aperture; VC, valine-citrulline, AA, alanine-alanine, NC, non-cleavable; Pan, panitumumab; NHS, *N*-hydroxy succinimide; DOL, degree of labeling; TBR, tumor-to-background ratio; TLR, liver-to-liver ratio; TMR, tumor-to-muscle ratio; IgG, immunoglobulin G; MeOH, methanol; SD, standard deviation.

ACKNOWLEDGMENT

This work was supported by the Intramural Research Program of the National Institutes of Health (NIH), NCI-CCR. It was also supported by an NCI CCR FLEX Program Award. The Biophysics Resource, CCR is acknowledged for use of instrumentation and assistance with mass spectrometry. Dr. Micheal Luciano is acknowledged for early studies developing SWIR ratiometric imaging. Dr. Freddy Escorcia (NIH/CCR) is acknowledged for helpful discussions and the obinutuzumab antibody. SMU acknowledges startup funds from The University of Texas at San Antonio, The Welch Foundation (AX-2216-20240404) and the Max and Minnie Tomerlin Voelcker Fund (SAT0004356). SMU acknowledges helpful conversation with Dr. Donald Caldwell and Dr. Kevin Burgess in the probe development phase. We thank Lisa Riffle (Small Animal Imaging Program), and Chelsea Sanders and Dr. Simone Difilippantonio (Laboratory Animal Sciences Program) for assistance with the *in vivo* study. This project has been funded in whole or in part with Federal funds from the National Cancer Institute, National Institutes of Health, under Contract No. HHSN261200800001E. The content of this publication does not necessarily reflect the views or policies of the Department of Health and Human Services, nor does mention of trade names, commercial products, or organizations imply endorsement by the U.S. Government.

REFERENCES

(1) Paul, S.; Konig, M. F.; Pardoll, D. M.; Bettegowda, C.; Papadopoulos, N.; Wright, K. M.; Gabelli, S. B.; Ho, M.; van Elsas, A.; Zhou, S. Cancer therapy with antibodies. *Nature reviews. Cancer* **2024**, *24*, 399.

(2) Owens, E. A.; Lee, S.; Choi, J.; Henary, M.; Choi, H. S. NIR fluorescent small molecules for intraoperative imaging. *Wiley Interdiscip Rev Nanomed Nanobiotechnol* **2015**, *7*, 828.

(3) Rosenthal, E. L.; Warram, J. M.; Bland, K. I.; Zinn, K. R. The status of contemporary image-guided modalities in oncologic surgery. *Ann Surg* **2015**, *261*, 46.

(4) Thapaliya, E. R.; Usama, S. M.; Patel, N. L.; Feng, Y.; Kalen, J. D.; St Croix, B.; Schnermann, M. J. Cyanine Masking: A Strategy to Test Functional Group Effects on Antibody Conjugate Targeting. *Bioconjug Chem* **2022**, *33*, 718.

(5) Usama, S. M.; Thapaliya, E. R.; Luciano, M. P.; Schnermann, M. J. Not so innocent: Impact of fluorophore chemistry on the in

https://doi.org/10.26434/chemrxiv-2024-zc58k **ORCID:** https://orcid.org/0000-0002-0503-0116 Content not peer-reviewed by ChemRxiv. **License:** CC BY-NC-ND 4.0

vivo properties of bioconjugates. *Curr Opin Chem Biol* **2021**, *63*, 38.
(6) Wei, W.; Rosenkrans, Z. T.; Liu, J.; Huang, G.; Luo, Q. Y.; Cai, W. ImmunoPET: Concept, Design, and Applications. *Chem Rev* **2020**, *120*, 3787.
(7) Sebastiano, J.; Samuels, Z. V.; Kao, W. S.; Zeglis, B. M. Site-specific bioconjugation and nuclear imaging. *Curr Opin Chem Biol* **2024**, *81*, 102471.
(8) Bruemmer, K. J.; Crossley, S. W. M.; Chang, C. J. Activity-Based Sensing: A Synthetic Methods Approach for Selective Molecular Imaging and Beyond. *Angewandte Chemie* **2020**, *59*, 13734.
(9) Hernandez Vargas, S.; Lin, C.; Tran Cao, H. S.; Ikoma, N.; AghaAmiri, S.; Ghosh, S. C.; Uselmann, A. J.; Azhdarinia, A. Receptor-Targeted Fluorescence-Guided Surgery With Low Molecular Weight Agents. *Front Oncol* **2021**, *11*, 674083.
(10) Wang, S.; Li, B.; Zhang, F. Molecular Fluorophores for Deep-Tissue Bioimaging. *ACS Cent Sci* **2020**, *6*, 1302.
(11) Schnermann, M. J.; Lavis, L. D. Rejuvenating old fluorophores with new chemistry. *Curr Opin Chem Biol* **2023**, *75*, 102335.
(12) Choi, H. S.; Gibbs, S. L.; Lee, J. H.; Kim, S. H.; Ashitate, Y.; Liu, F.; Hyun, H.; Park, G.; Xie, Y.; Bae, S.; Henary, M.; Frangioni, J. V. Targeted zwitterionic near-infrared fluorophores for improved optical imaging. *Nat Biotechnol* **2013**, *31*, 148.
(13) Bhattacharyya, S.; Patel, N.; Wei, L.; Riffle, L. A.; Kalen, J. D.; Hill, G. C.; Jacobs, P. M.; Zinn, K. R.; Rosenthal, E. Synthesis and biological evaluation of panitumumab-IRDye800 conjugate as a fluorescence imaging probe for EGFR-expressing cancers. *Medchemcomm* **2014**, *5*, 1337.
(14) Scott, J. I.; Deng, Q.; Vendrell, M. Near-Infrared Fluorescent Probes for the Detection of Cancer-Associated Proteases. *Acs Chem Biol* **2021**, *16*, 1304.
(15) Mc Larney, B. E.; Kim, M.; Roberts, S.; Skubal, M.; Hsu, H. T.; Ogirala, A.; Pratt, E. C.; Pillarsetty, N. V. K.; Heller, D. A.; Lewis, J. S.; Grimm, J. Ambient Light Resistant Shortwave Infrared Fluorescence Imaging for Preclinical Tumor Delineation via the pH Low-Insertion Peptide Conjugated to Indocyanine Green. *J Nucl Med* **2023**, *64*, 1647.
(16) Hu, Z.; Fang, C.; Li, B.; Zhang, Z.; Cao, C.; Cai, M.; Su, S.; Sun, X.; Shi, X.; Li, C.; Zhou, T.; Zhang, Y.; Chi, C.; He, P.; Xia, X.; Chen, Y.; Gambhir, S. S.; Cheng, Z.; Tian, J. First-in-human liver-tumour surgery guided by multispectral fluorescence imaging in the visible and near-infrared-I/II windows. *Nat Biomed Eng* **2020**, *4*, 259.
(17) Carr, J. A.; Franke, D.; Caram, J. R.; Perkinson, C. F.; Saif, M.; Askoxylakis, V.; Datta, M.; Fukumura, D.; Jain, R. K.; Bawendi, M. G.; Bruns, O. T. Shortwave infrared fluorescence imaging with the clinically approved near-infrared dye indocyanine green. *Proc Natl Acad Sci U S A* **2018**, *115*, 4465.
(18) Yin, Q.; You, S. L. Intramolecular alkene electrophilic bromination initiated ipso-bromocyclization for the synthesis of functionalized azaspirocyclohexadienones. *Org Lett* **2012**, *14*, 3526.
(19) Cosco, E. D.; Spearman, A. L.; Ramakrishnan, S.; Lingg, J. G. P.; Saccomano, M.; Pengshung, M.; Arus, B. A.; Wong, K. C. Y.; Glasl, S.; Ntziachristos, V.; Warmer, M.; McLaughlin, R. R.; Bruns, O. T.; Sletten, E. M. Shortwave infrared polymethine fluorophores matched to excitation lasers enable non-invasive, multicolour in vivo imaging in real time. *Nat Chem* **2020**, *12*, 1123.
(20) Alarcon, E. I.; Poblete, H.; Roh, H.; Couture, J. F.; Comer, J.; Kochevar, I. E. Rose Bengal Binding to Collagen and Tissue Photobonding. *Acs Omega* **2017**, *2*, 6646.
(21) Bandi, V. G.; Luciano, M. P.; Saccomano, M.; Patel, N. L.; Bischof, T. S.; Lingg, J. G. P.; Tsrunchev, P. T.; Nix, M. N.; Ruehle, B.; Sanders, C.; Riffle, L.; Robinson, C. M.; Difilippantonio, S.; Kalen, J. D.; Resch-Genger, U.; Ivanic, J.; Bruns, O. T.; Schnermann, M. J. Targeted multicolor in vivo imaging over 1,000 nm enabled by nonamethine cyanines. *Nat Methods* **2022**, *19*, 353.
(22) Cosco, E. D.; Caram, J. R.; Bruns, O. T.; Franke, D.; Day, R. A.; Farr, E. P.; Bawendi, M. G.; Sletten, E. M. Flavylium Polymethine Fluorophores for Near- and Shortwave Infrared Imaging. *Angewandte Chemie* **2017**.
(23) Li, B. H.; Zhao, M. Y.; Zhang, F. Rational Design of Near-Infrared-II Organic Molecular Dyes for Bioimaging and Biosensing. *Acs Mater Lett* **2020**, *2*, 905.
(24) Zhang, X.; Li, S.; Ma, H.; Wang, H.; Zhang, R.; Zhang, X. D. Activatable NIR-II organic fluorescent probes for bioimaging. *Theranostics* **2022**, *12*, 3345.
(25) Thurber, G. M.; Schmidt, M. M.; Wittrup, K. D. Factors determining antibody distribution in tumors. *Trends Pharmacol Sci* **2008**, *29*, 57.
(26) Lee, B. C.; Chalouni, C.; Doll, S.; Nalle, S. C.; Darwish, M.; Tsai, S. P.; Kozak, K. R.; Del-Rosario, G.; Yu, S. F.; Erickson, H.; Vandlen, R. FRET Reagent Reveals the Intracellular Processing of Peptide-Linked Antibody-Drug Conjugates. *Bioconjug. Chem.* **2018**, *29*, 2468.
(27) Thankarajan, E.; Jadhav, S.; Luboshits, G.; Gellerman, G.; Patsenker, L. Quantification of Drug Release Degree In Vivo Using Antibody-Guided, Dual-NIR-Dye Ratiometric System. *Anal Chem* **2021**, *93*, 8265.
(28) Poplinger, D.; Bokan, M.; Hesin, A.; Thankarajan, E.; Tuchinsky, H.; Gellerman, G.; Patsenker, L. Ratiometric Fluorescence Monitoring of Antibody-Guided Drug Delivery to Cancer Cells. *Bioconjug. Chem.* **2021**, *32*, 1641.
(29) Sorkin, M. R.; Walker, J. A.; Kabaria, S. R.; Torosian, N. P.; Alabi, C. A. Responsive Antibody Conjugates Enable Quantitative Determination of Intracellular Bond Degradation Rate. *Cell Chem Biol* **2019**, *26*, 1643.
(30)Miltsov, S.; Encinas, C.; Alonso, J. N. Nortricarbocyanines: New near-infrared pH-indicators. Tetrahedron Lett. 1998, 39 (50),9253−9254.
(31) Zhang, Z. R.; Achilefu, S. Design, synthesis and evaluation of near-infrared fluorescent pH indicators in a physiologically relevant range. *Chem Commun* **2005**, 5887.
(32) Lee, H.; Akers, W.; Bhushan, K.; Bloch, S.; Sudlow, G.; Tang, R.; Achilefu, S. Near-infrared pH-activatable fluorescent probes for imaging primary and metastatic breast tumors. *Bioconjug Chem* **2011**, *22*, 777.

(33) Thavornpradit, S.; Usama, S. M.; Park, G. K.; Shrestha, J. P.; Nomura, S.; Baek, Y.; Choi, H. S.; Burgess, K. QuatCy: A Heptamethine Cyanine Modification With Improved Characteristics. *Theranostics* **2019**, *9*, 2856.
(34) Qian, H.; Cheng, Q.; Tian, Y.; Dang, H.; Teng, C.; Yan, L. An anti-aggregation NIR-II heptamethine-cyanine dye with a stereo-specific cyanine for imaging-guided photothermal therapy. *J Mater Chem B* **2021**, *9*, 2688.
(35) Usama, S. M.; Caldwell, D. R.; Shrestha, P.; Luciano, M. P.; Patel, N. L.; Kalen, J. D.; Ivanic, J.; Schnermann, M. J. Modified norcyanines enable ratiometric pH imaging beyond 1000 nm. *Biosens Bioelectron* **2022**, *217*, 114610.
(36) Tao, Z. M.; Hong, G. S.; Shinji, C.; Chen, C. X.; Diao, S.; Antaris, A. L.; Zhang, B.; Zou, Y. P.; Dai, H. J. Biological Imaging Using Nanoparticles of Small Organic Molecules with

https://doi.org/10.26434/chemrxiv-2024-zc58k **ORCID:** https://orcid.org/0000-0002-0503-0116 Content not peer-reviewed by ChemRxiv. **License:** CC BY-NC-ND 4.0

Fluorescence Emission at Wavelengths Longer than 1000 nm. *Angew Chem Int Edit* **2013**, *52*, 13002.
(37) Lei, Z.; Sun, C.; Pei, P.; Wang, S.; Li, D.; Zhang, X.; Zhang, F. Stable, Wavelength-Tunable Fluorescent Dyes in the NIR-II Region for In Vivo High-Contrast Bioimaging and Multiplexed Biosensing. *Angewandte Chemie* **2019**, *58*, 8166.
(38) Garcia-Foncillas, J.; Sunakawa, Y.; Aderka, D.; Wainberg, Z.; Ronga, P.; Witzler, P.; Stintzing, S. Distinguishing Features of Cetuximab and Panitumumab in Colorectal Cancer and Other Solid Tumors. *Front Oncol* **2019**, *9*, 849.
(39) Luciano, M. P.; Crooke, S. N.; Nourian, S.; Dingle, I.; Nani, R. R.; Kline, G.; Patel, N. L.; Robinson, C. M.; Difilippantonio, S.; Kalen, J. D.; Finn, M. G.; Schnermann, M. J. A Nonaggregating Heptamethine Cyanine for Building Brighter Labeled Biomolecules. *Acs Chem Biol* **2019**, *14*, 934.
(40) Usama, S. M.; Marker, S. C.; Li, D. H.; Caldwell, D. R.; Stroet, M.; Patel, N. L.; Tebo, A. G.; Hernot, S.; Kalen, J. D.; Schnermann, M. Method To Diversify Cyanine Chromophore Functionality Enables Improved Biomolecule Tracking and Intracellular Imaging. *J Am Chem Soc* **2023**, *145*, 14647.
(41) Huang, X.; Song, J.; Yung, B. C.; Huang, X.; Xiong, Y.; Chen, X. Ratiometric optical nanoprobes enable accurate molecular detection and imaging. *Chem Soc Rev* **2018**, *47*, 2873.
(42) Yazaki, P.; Lwin, T.; Minnix, M.; Li, L.; Sherman, A.; Molnar, J.; Miller, A.; Frankel, P.; Chea, J.; Poku, E.; Bowles, N.; Hoffman, R.; Shively, J.; Bouvet, M. Improved antibody-guided surgery with a near-infrared dye on a pegylated linker for CEA-positive tumors. *J Biomed Opt* **2019**, *24*, 1.
(43) Matikonda, S. S.; McLaughlin, R.; Shrestha, P.; Lipshultz, C.; Schnermann, M. J. Structure-Activity Relationships of Antibody-Drug Conjugates: A Systematic Review of Chemistry on the Trastuzumab Scaffold. *Bioconjug Chem* **2022**, *33*, 1241.
(44) Beck, A.; Goetsch, L.; Dumontet, C.; Corvaia, N. Strategies and challenges for the next generation of antibody-drug conjugates. *Nat Rev Drug Discov* **2017**, *16*, 315.
(45) Usama, S. M.; Marker, S. C.; Caldwell, D. R.; Patel, N. L.; Feng, Y.; Kalen, J. D.; St Croix, B.; Schnermann, M. J. Targeted Fluorogenic Cyanine Carbamates Enable In Vivo Analysis of Antibody-Drug Conjugate Linker Chemistry. *J Am Chem Soc* **2021**, *143*, 21667.
(46) Sato, K.; Nagaya, T.; Nakamura, Y.; Harada, T.; Nani, R. R.; Shaum, J. B.; Gorka, A. P.; Kim, I.; Paik, C. H.; Choyke, P. L.; Schnermann, M. J.; Kobayashi, H. Impact of C4'-O-Alkyl Linker on in Vivo Pharmacokinetics of Near-Infrared Cyanine/Monoclonal Antibody Conjugates. *Mol Pharm* **2015**, *12*, 3303.
(47) Sato, K.; Gorka, A. P.; Nagaya, T.; Michie, M. S.; Nakamura, Y.; Nani, R. R.; Coble, V. L.; Vasalatiy, O. V.; Swenson, R. E.; Choyke, P. L.; Schnermann, M. J.; Kobayashi, H. Effect of charge localization on the in vivo optical imaging properties of near-infrared cyanine dye/monoclonal antibody conjugates. *Mol Biosyst* **2016**, *12*, 3046.
(48) Senter, P. D.; Sievers, E. L. The discovery and development of brentuximab vedotin for use in relapsed Hodgkin lymphoma and systemic anaplastic large cell lymphoma. *Nat Biotechnol* **2012**, *30*, 631.
(49) Salomon, P. L.; Reid, E. E.; Archer, K. E.; Harris, L.; Maloney, E. K.; Wilhelm, A. J.; Miller, M. L.; Chari, R. V. J.; Keating, T. A.; Singh, R. Optimizing Lysosomal Activation of Antibody-Drug Conjugates (ADCs) by Incorporation of Novel Cleavable Dipeptide Linkers. *Mol Pharm* **2019**, *16*, 4817.
(50) Wang, Y.; Fan, S.; Zhong, W.; Zhou, X.; Li, S. Development and Properties of Valine-Alanine based Antibody-Drug Conjugates with Monomethyl Auristatin E as the Potent Payload. *Int J Mol Sci* **2017**, *18*.
(51) Dal Corso, A.; Cazzamalli, S.; Gebleux, R.; Mattarella, M.; Neri, D. Protease-Cleavable Linkers Modulate the Anticancer Activity of Noninternalizing Antibody-Drug Conjugates. *Bioconjug Chem* **2017**, *28*, 1826.
(52) Cazzamalli, S.; Corso, A. D.; Neri, D. Linker stability influences the anti-tumor activity of acetazolamide-drug conjugates for the therapy of renal cell carcinoma. *J Control Release* **2017**, *246*, 39.
(53) Jeffrey, S. C.; Nguyen, M. T.; Andreyka, J. B.; Meyer, D. L.; Doronina, S. O.; Senter, P. D. Dipeptide-based highly potent doxorubicin antibody conjugates. *Bioorg Med Chem Lett* **2006**, *16*, 358.
(54) Xu, L.; Packer, L. E.; Qian, M. G.; Wu, J. T. Rapid quantification of a cleavable antibody-conjugated drug by liquid chromatography/tandem mass spectrometry with microwave-assisted enzymatic cleavage. *J Pharm Biomed Anal* **2016**, *128*, 226.
(55) Bessire, A. J.; Ballard, T. E.; Charati, M.; Cohen, J.; Green, M.; Lam, M. H.; Loganzo, F.; Nolting, B.; Pierce, B.; Puthenveetil, S.; Roberts, L.; Schildknegt, K.; Subramanyam, C. Determination of Antibody-Drug Conjugate Released Payload Species Using Directed in Vitro Assays and Mass Spectrometric Interrogation. *Bioconjug Chem* **2016**, *27*, 1645.
(56) Cilliers, C.; Nessler, I.; Christodolu, N.; Thurber, G. M. Tracking Antibody Distribution with Near-Infrared Fluorescent Dyes: Impact of Dye Structure and Degree of Labeling on Plasma Clearance. *Mol Pharm* **2017**, *14*, 1623.
(57) Bordeau, B. M.; Balthasar, J. P. Strategies to enhance monoclonal antibody uptake and distribution in solid tumors. *Cancer Biol Med* **2021**, *18*, 649.
(58) Pereira, P. M. R.; Mandleywala, K.; Ragupathi, A.; Lewis, J. S. Acute Statin Treatment Improves Antibody Accumulation in EGFR- and PSMA-Expressing Tumors. *Clin Cancer Res* **2020**, *26*, 6215.

https://doi.org/10.26434/chemrxiv-2024-zc58k **ORCID:** https://orcid.org/0000-0002-0503-0116 Content not peer-reviewed by ChemRxiv. **License:** CC BY-NC-ND 4.0